Drug Design, Development and Therapy

Dovepress

open access to scientific and medical research

Open Access Full Text Article

ORIGINAL RESEARCH

Binary Nanodrug-Delivery System Designed for Leukemia Therapy: Aptamer- and Transferrin-Codecorated Daunorubicin- and Luteolin-Coloaded Nanoparticles

Yuanyuan Zhu, Wei Zhang, Jing Chen

Department of Pharmacy, Qingdao Hospital of Traditional Chinese Medicine, Qingdao Hiser Hospital Affiliated with Qingdao University, Qingdao, Shandong Province, People's Republic of China

Correspondence: Jing Chen, Department of Pharmacy, Qingdao Hospital of Traditional Chinese Medicine, Qingdao Hiser Hospital Affiliated with Qingdao University, 4 Renmin Road, Qingdao, Shandong Province, 266000, People's Republic of China, Email chenjingqdu@outlook.com

Objective: This study aimed to develop a binary nanodrug-delivery system decorated with aptamers (APs) and transferrin (Tf) and loaded with daunorubicin (Drn) and luteolin (Lut) for the treatment of leukemia.

Methods: Oligonucleotide AP- and Tf-contaiing ligands were designed and synthesized separately. AP-decorated Drn-loaded nanoparticles (AP-Drn NPs) and Tf-Lut NPs were prepared by self-assembly. An AP- and Tf-codecorated Drn- and Lut-coloaded nanodrug-delivery system (AP/Tf-Drn/Lut NPs) was prepared by self-assembly of AP-Drn NPs and Tf-Lut NPs. In vitro and in vivo efficiency of the system was evaluated on leukemia cell line and cell-bearing mouse model in comparison with single ligand–decorated, single drug–loaded and free-drug formulations.

Results: AP/Tf-Drn/Lut NPs were spherical and nanosized (187.3±5.3 nm) and loaded with about 85% of drugs. In vitro cytotoxicity of AP/Tf-Drn/Lut NPs was remarkably higher than single ligand–decorated ones. Double drug–loaded AP/Tf-Drn/Lut NPs exhibited higher tumor-cell inhibition than single drug–loaded ones, which showed a synergic effect of the two drugs. AP/Tf-Drn/Lut NPs achieved the most efficient antileukemic activity and absence of toxicity in vivo.

Conclusion: The present study showed that AP/Tf-Drn/Lut NPs are a promising drug-delivery system for targeted treatment of leukemia, due to the synergic effect of the two drugs in this system. The limitations of this system include stability during large-scale production and application from bench to bedside.

Keywords: acute myeloid leukemia, daunorubicin, luteolin, aptamer, transferrin, nanodrug-delivery system

Introduction

Acute myeloid leukemia (AML), a heterogeneous hematologic malignancy, is the most common acute leukemia among adults.[1] Clinical outcomes of patients with AML are still poor, with <30% surviving 5 years and higher incidence and an almost 90% mortality rate for older patients (>65 years).[2,3] Current treatmentsfor AML mainly consist of standard chemotherapy (a combination of cytarabine and daunorubicin [Drn] or idarubicin), targeted therapy using FLT3 inhibitors, including midostaurin, quizartinib, and cabozantinib, and immunotherapy, eg, gemtuzumab ozogamicin (anti-CD33 monoclonal antibody conjugated with calicheamicin).[3–6] Unfortunately, current treatments still have therapeutic obstacles, including lower compliance, because of serious toxicity and therapeutic efficacy due to drug resistance. Therefore, it is urgent to exploit new therapeutic strategies to improve treatment outcomes.

Nanoparticle (NP)-based combination therapy has attracted extensive attention in recent years for AML therapy. Currently, there are two liposomal formulations available in the clinic for the treatment of HM (liposomal Drn [DaunoXome] and liposomal cytarabine + Drn [CPX-351/VYXEOS]).[7,8] Phase III results have proven that compared to free drug (Drn and cytarabine), the liposomal formulation codelivering Drn and cytarabine significantly

Received: 30 August 2022
Accepted: 15 December 2022
Published: 6 January 2023

improves median overall survival (9.56 vs 5.95 months) and overall remission rate (47.7% vs 33.3%) for elderly patients with newly diagnosed high-risk secondary AML.[9] This brings forth a new era for AML patients based on Drn-combination nanoformulation therapy.

An anthracycline topoisomerase inhibitor, Drn is a broad-spectrum antihematologic malignancy agent for AML, acute nonlymphocytic leukemia of adults, and acute lymphocytic leukemia of children and adults.[10] However, multidrug resistance hampered the further clinical application of Drn injections. Recently, Chinese herbal medicine and NPs have attracted research interest to overcome multidrug resistance.[11,12] Luteolin (Lut; 3′,4′,5,7-tetrahydroxyflavone) has been applied in traditional Chinese medicine for treating various diseases, including inflammatory disorders, angiocardiopathy, and cancer.[13,14] Various studies have demonstrated that Lut has the ability to enhance the antileukemia capacity of chemotherapeutic agents and anti–multidrug resistance by upregulation of P-gp and BCL2, downregulation of MCL1 expression, and inducing apoptosis of HL60 cells that was associated with c-Jun activation and histone H3 acetylation–mediated Fas/FasL expression.[15–18] We were unable to find literature any on combination leukemia treatment using Drn and Lut together in one nanoformulation. Therefore, combination treatment with Drn and Lut is anticipated in our study to provide better outcomes in terms of cytotoxicity and less multidrug resistance.

Aptamers (APs) can recognize their targets with high specificity and affinity, and AP-mediated targeting systems have been demonstrated to have great potential for AML therapy.[19] Oligonucleotide APs can specifically bind to biomarkers on AML cells, on which the biomarker CD117 is highly expressed.[20] Also, AML cells are known to overexpress a number of cell-surface proteins including transferrin (Tf) receptors. Tf receptor–targeted drug delivery to tumor cells can be achieved by conjugation of the ligand Tf to the surface of NPs.[21] Polyethylene glycol (PEG) is a kind of polymer that can be used as a linker for covalent attachment of various ligands. The free end of a PEG chain can be functionalized to reactive amine, carboxylic acid, or sulfhydryl groups, then the wide assortment of ligands can be efficiently covalently attached to the PEG chain by amide bonding or disulfide-bridge formation.[22] PEG was used as a linker to achieve AP and Tf decoration in this study.

In this paper, an AP- and Tf-codecorated, Drn- and Lut-coloaded binary nanodrug-delivery system (AP/Tf-Drn/Lut NPs) was designed for AML therapy. In vitro and in vivo efficiency of the system was evaluated on a leukemia cell line and cell-bearing mouse model in comparison with single ligand–decorated, single drug–loaded, and free-drug formulations.

Methods

Materials

Drn, Lut, oleic acid (OA), phosphatidylglycerol, human Tf (iron-free), and *N*-hydroxysuccinimide (NHS) were purchased from Sigma (St Louis, MO, USA) and (2,3-dioleoyloxy-propyl)-trimethylammonium (DOTAP) was provided by Avanti Polar Lipids (Birmingham, AL, USA). PEG-COOH (NH_2-PEG-COOH) and DSPE-PEG-COOH were obtained from Ponsure Biological (Shanghai, China). The human leukocyte cell line HL60 was obtained from the American Type Culture Collection (Manassas, VA) and cultured in Dulbecco's modified Eagle's medium (DMEM) supplemented with 10% FBS at 37°C in a 5% CO_2 incubator.

Animals

BALB/c nude mice (female, 4–6 weeks old) were purchased from Beijing Vital River Laboratory Animal Technology (Beijing, China), and in vivo animal experiments were performed followed the National Institutes of Health *Guide for the Care and use of Laboratory Animals*. The Animal Ethics Committee of Qingdao Hospital of Traditional Chinese Medicine approved the animal experiments.

Synthesis of AP–Polyethylene Glycol–Oleic Acid

Firstly, PEG-OA was synthesized as follows. NH_2-PEG-COOH and TEA were dissolved in DMSO, then added to an OA, DCC, and NHS mixture in DMSO under stirring for 12 h at room temperature.[20] OA-PEG-COOH was purified by filtration. Then, CD117-specific AP was conjugated with OA-PEG-COOH to form AP-PEG-OA conjugates. OA-PEG-COOH was activated by NHS and then reacted with a 5'-terminal amino-modified oligonucleotide CD117-specific AP

containing a functional amino group. The reaction solution was mixed overnight at room temperature, then purified by high-performance liquid chromatography (HPLC) and dried by lyophilization to obtain AP-PEG-OA conjugates as pale-white solids and confirmed by an enhanced BCA protein assay kit at 562 nm.

Synthesis of Tf-PEG-DSPE

Tf-PEG-DSPE was synthesized by forming an amide linkage between Tf and DSPE-PEG-COOH.[21] DSPE-PEG-COOH, DCC and NHS were dissolved in DMSO and stirred for 10 h, then Tf and TEA were added. The reaction mixture was stirred for 10 h under a nitrogen atmosphere at room temperature and filtered. Tf-PEG-DSPE was obtained by dialyzing and lyophilizing. The structure of Tf-PEG-PE was confirmed by infrared and ^{1}H NMR spectroscopy.

Preparation of Nanodrug-Delivery System

AP-decorated, Drn-loaded (AP-Drn) NPs (Figure 1A) and Tf-Lut NPs, Figure 1A) were prepared by thin-film dispersion.[23] For AP-Drn NPs, AP-PEG-OA (200 mg) and Drn (100 mg) were dissolved in acetone (5 mL), then the acetone was slowly removed under reduced pressure in a hot-water bath (60°C) to form a thin film. Then, deionized water containing DOTAP (0.5%, w/v) was added to the film and AP-Drn NPs obtained by hydration. For Tf-Lut NPs, Tf-PEG-DSPE (200 mg), Lut (100 mg), and phosphatidylglycerol (20 mg) were dissolved in acetone (5 mL) and the acetone slowly removed under reduced pressure in a hot-water bath (60°C) to form a thin film. Then, deionized water was added to the film and AP-Drn NPs obtained by hydration.

AP/Tf-Drn/Lut NPs (Figure 1A) were prepared by self-assembly.[22] AP-Drn NPs were added to Tf-Lut NPs under stirring (400 rpm). The AP- and Tf-codecorated binary nanodrug-delivery system without drug (AP/Tf NPs) was prepared using no drug. Single AP- or Tf-decorated Drn- and Lut-coloaded nanodrug-delivery systems (AP-Drn/Lut NPs or Tf-Drn/Lut NPs) were prepared using PEG-OA instead of AP-PEG-OA or PEG-DSPE instead of Tf-PEG-DSPE. The resulting NP systems were lyophilized at and stored at 4°C.

Characterization of Nanodrug-Delivery System

The surface morphology of AP-Drn NPs, Tf-Lut NPs, and AP/Tf-Drn/Lut NPs was observed by negative staining with one drop of a 3% aqueous solution of sodium phosphotungstate and then examined with

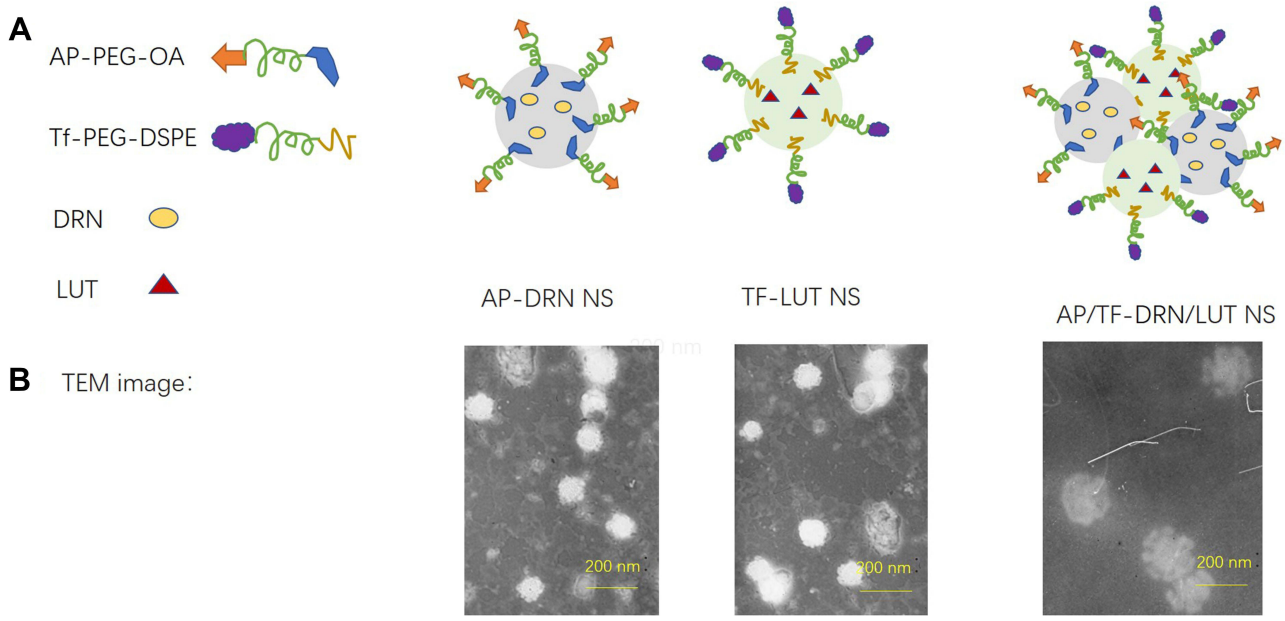

Figure 1 Scheme (**A**) and TEM images (**B**) of AP/Tf-Drn/Lut NPs.
Note: AP/Tf-Drn/Lut NPs were nanosized with some ligands on the spherical surface.

transmission electron microscopy (JEOL, Tokyo, Japan).[24] The size of nanodrug-delivery systems was characterized with dynamic light scattering (Beckman Coulter Delsa Nano C, Fullerton, CA) and ?-potential was tested using a Zetasizer (Malvern Instruments, Malvern, UK). Drn and Lut encapsulation efficiency (EE) and loading content (LC) were analyzed by HPLC using a C_{18} column (150×4.6 mm, 12 nm): mobile phase 0.01 M KH_2PO_4–acetonitrile–acetic acid (45:55:0.27 v:v:v, 0.5 mL/min, detector wavelength 350 and 490 nm for Lut and Drn, respectively.[25,26]

Stability of Nanodrug-Delivery System

The stability of AP-Drn NPs, Tf-Lut NPs, and AP/Tf-Drn/Lut NPs in PBS and culture medium (DMEM supplemented with 10% FBS) was investigated by mixing the nanodrug-delivery systems (20 mg) with PBS or culture medium (10 mL) at pH 7.4 and incubated at 37°C for 4 days.[27] Changes in particle size and EE were analyzed using the same aforementioned methods.

In Vitro Release Assays

In vitro drug release from nanosystems was evaluated by dialysis in dialysis bags (molecular weight cutoff 3500 Da).[28] AP/Tf-Drn/Lut NPs, AP-Drn/Lut NPs, Tf-Drn/Lut NPs, AP-Drn NPs, and Tf-Lut NPs were sealed in the dialysis bags separately (1 mL each) and placed in PBS (20 mL) containing 0.5% Tween 80, stirred (100 rpm), and incubated (37°C). Samples (200 μL) were taken from the release buffer at determined time points and an equal amount of fresh buffer was added after sampling. The content of Drn and Lut in the samples was determined by HPLC.

Cellular Uptake

To assess the cellular uptake of NPs, coumarin 6 was added along with the drugs as described in the "Preparation of nanodrug-delivery system" section.[29] HL60 cells were cultured in a 24-well plate (10^5 cells/well) and nanodrug-delivery systems added and incubated for 1 and 24 h. Then, the cells were washed three times with D-Hank's solution, collected and centrifuged, and uptake efficiency quantified using a BD FACSCalibur flow cytometer.

Cytotoxicity Assays

The cytotoxicity of AP/Tf-Drn/Lut NPs and other formulations was evaluated with MTS assays.[30] The HL60 cells were cultured in a 96-well plate overnight and the culture medium replaced with fresh medium. AP/Tf-Drn/Lut NPs, AP-Drn /Lut NPs, Tf-Drn/Lut NPs, AP-Drn NPs, Tf-Lut NPs, free Drn/Lut, free Drn, and free Lut were incubated with the cells for 48 h. MTS solution (15 μL) was then added to each well and incubated for a further 4 h at 37°C. Cell viability was evaluated by a microplate reader at 490 nm. Cell-survival rates were calculated as normalized to untreated control wells.

Drug Combination

The synergic effect of Drn and Lut combinations was evaluated with the combination index (CI) using the Chou–Talalay method.[31] The CI of drug concentration causing 50% inhibition (CI_{50}) was measured with the equation $CI_{50} = (D)_{Drn}/(D_{50})_{Drn} + (D)_{Lut}/(D_{50})_{Lut}$. $(D)_{Drn}$ and $(D)_{Lut}$ are the concentration of Drn and Lut in the combination system (AP/Tf-Drn /Lut NPs) when 50% cytotoxicity was achieved, $(D_{50})_{Drn}$ and $(D_{50})_{Lut}$ represent the concentration of single drug (AAP-Drn NPs or Tf-Lut NPs) exhibiting 50% cytotoxicity. CI_{50} <1, 1, and >1 illustrate synergy, additive, and antagonism in drug combinations, respectively.

In Vivo AML-Therapy Efficiency

HL60 cells (10^6 cells in 150 μL PBS) were injected subcutaneously into the left flank of BALB/c nude mice to produce the murine leukemia model. Tumor size was measured with a caliper and determined: $L \times W^2/2$ (L, longest side of the tumor; W, widest side vertical to L).[32] After tumor growth to about 100 mm^3, mice were randomly divided into ten groups (n=8), then AP/Tf-Drn/Lut NPs (Drn 5 mg and Lut 2 mg per kg), AP-Drn/Lut NPs (Drn 5 mg and Lut 2 mg per kg), Tf-Drn/Lut NPs (Drn 5 mg and Lut 2 mg per kg), AP-Drn NPs (Drn 10 mg per kg), Tf-Lut NPs (Lut 4 mg per kg), AP/Tf NPs, free Drn/Lut (Drn 5 mg and Lut 2 mg per kg), free Drn (10 mg per kg), free Lut (4 mg per kg), and 0.9% saline solution were intravenously injected in the mice on days 0, 3, 6, 9, 12, 15, 18, and 21. The body weight of

mice was monitored throughout the 21 days. Blood chemistry — creatinine (Cre; kidney function), alanine aminotransferase (ALT; liver function) and white blood cells (WBCs) — was also evaluated.

In Vivo Pharmacokinetics and Biodistribution

Mice were randomly divided randomly divided into four groups (n=8), then AP/Tf-Drn/Lut NPs, AP-Drn/Lut NPs, Tf-Drn /Lut NPs, and free Drn/Lut (each containing Drn 5 mg and/or Lut 2 mg per kg) were intravenously injected.[33] Blood was collected in heparinized tubes at determined time points and centrifuged (1000 *g* for 10 min), plasma separated, triple methanol added, and then centrifuged (1000 *g* for 5 min). Heart, liver, lung, kidney, spleen, bone marrow, and tumor tissue were harvested after 1 and 48 h and homogenized with saline. Bone marrow was titrated from the femur and tibia bones with RPMI media (Gibco) containing 5% FBS using a 28-gauge syringe.[34] Hexane–diethyl ether (3:1, v:v) was then added to extract the drugs from the tissue, centrifuged (1000 *g* for 10 min), and the upper layer collected. The drug contents in the tissue and blood were analyzed by the methods in the "Characterization of nanodrug-delivery system" section.

Statistical Analysis

Results are presented as means ± SD. The significance of differences was assessed using unpaired *t* tests (between two groups) or one-way ANOVA (among three or more groups) using SPSS 19.0. Significance was taken as $P<0.05$.

Results

Characterization of AP-PEG-OA and Tf-PEG-DSPE

Absorbance of the eluates of AP-PEG-OA and free AP was measured using an enhanced BCA protein assay kit at 562 nm separately to confirm that the AP had been linked to PEG-OA. There was one peak during 12 to 15 min for free AP, while there were two peaks for AP-PEG-OA. One overlapped the peak of free AP, demonstrating successful linking of AP to PEG-OA. The formation of Tf-PEG-DSPE was confirmed by infrared (IR) and ^{1}H NMR spectroscopy. IR: 3621.3 (–NH–, –OH), 1898.5 (–C=O), 1665.1 (–HN–CO–), 1621.7 (–HN–CO–). ^{1}H NMR ($CDCl_3$, 300 MHz) δ (ppm): 0.89 ($–CH_3$), 1.12–1.97 (DSPE protons), 2.33 ($–COCH_2–$), 2.42 ($–COCH_2CH_2–$), 2.61 ($–CH_2N–$), 3.39 ($–OCH_3–$), 3.70–4.10 (PEG protons), 5.82 (–NH–). The yields of AP-PEG-OA and Tf-PEG-DSPE were 73.9% and 78.6%, respectively.

Characterization of Nanodrug-Delivery System

AP/Tf-Drn/Lut NPs, AP-Drn NPs, and Tf-Lut NPs were spherical (Figure 1B). The size of AP/Tf-Drn/Lut NPs was 187.3±5.3 nm (Table 1), while AP-Drn NPs (91.5±2.8 nm) and Tf-Lut NPs (88.7±2.5 nm) were smaller. Besides positively charged AP-Drn NPs (18.9±1.7 mV), all the other samples tested showed negative charge (?-potential). The EE of AP/Tf-Drn/Lut NPs and other samples was >85%. The size and EE of AP/Tf-Drn/Lut NPs, AP-Drn NPs, and Tf-Lut NPs showed no obvious change during the 4 days of the study (Figure 2A and B), which is similar to the finding of Chen et al,[35] proving the stability of these systems.

Table 1 Characterization of nanodrug-delivery systems (means ± SD, n=3)

Formulations	Particle size (nm)	PDI	ζ-potential (mV)	Drn		Lut	
				EE (%)	LC (%)	EE (%)	LC (%)
AP/Tf-Drn/Lut NPs	187.3±5.3	0.142±0.019	−25.4±2.6	88.7±3.9	5.2±0.5	85.9±4.2	2.1±0.4
AP-Drn/Lut NPs	186.7±4.7	0.139±0.023	−19.2±2.1	87.5±3.8	5.9±0.6	86.7±3.7	2.4±0.6
Tf-Drn/Lut NPs	188.3±4.5	0.126±0.016	−17.5±1.8	86.5±4.1	5.7±0.6	88.3±3.9	2.2±0.5
AP-Drn NPs	91.5±2.8	0.112±0.011	+18.9±1.7	89.4±4.4	11.8±1.1	/	/
Tf-Lut NPs	88.7±2.5	0.128±0.014	−38.9±3.1	/	/	86.5±3.6	4.6±0.7
AP/Tf NPs	187.8±5.1	0.147±0.026	−37.6±2.9	/	/	/	/

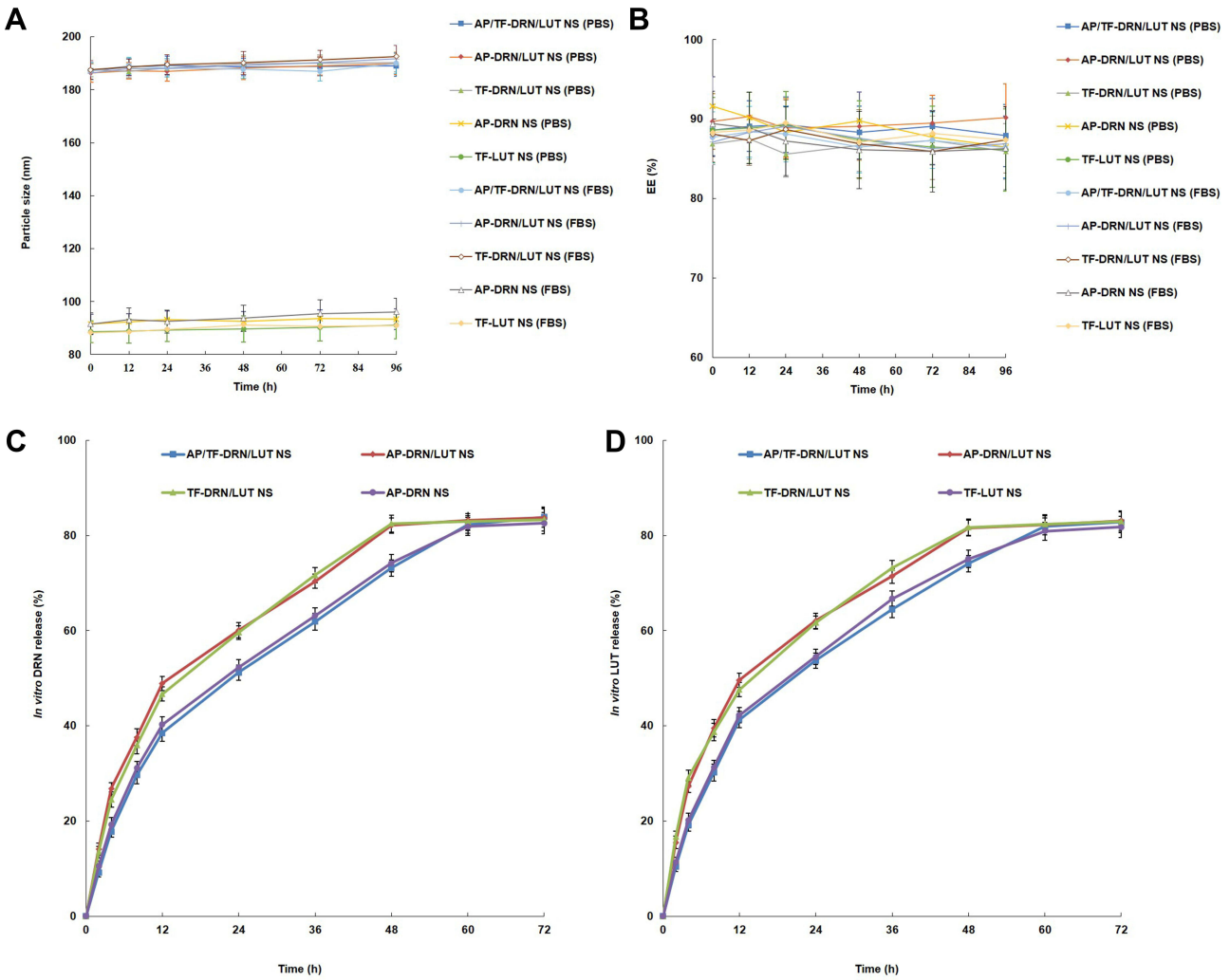

Figure 2 Changes in particle size (**A**) and EE (**B**) analyzed in PBS and culture medium (FBS). In vitro drug-release behavior of Drn (**C**) or Lut (**D**) from nanosystems evaluated by dialysis.
Notes: Sustained drug-release patterns were found for all the samples tested. Data presented as means ± SD, n=3.

In Vitro Release Assays

Sustained drug-release patterns were found for all the samples tested (Figure 2C and D). Drug release from dual ligand–codecorated AP/Tf-Drn/Lut NPs was slower than single ligand (AP or Tf)–decorated systems. Take Drn release as an example. We can tell from Figure 2C that AP/Tf-Drn/Lut NPs and AP-Drn NPs exhibited complete Drn release after 60 h, while AP-Drn/Lut NPs and Tf-Drn/Lut NPs took 48 h.

Cellular Uptake

The cellular uptake of the nanosystems is summarized in Table 2 and Supplement Figure 1. All nanosystems tested showed high uptake efficiency at 1 and 24 h. Dual liganddecorated AP/Tf-Drn/Lut NPs and AP/Tf NPs showed higher uptake than single ligand–modified ones ($P<0.05$), which may be evidence of the targeting ability of these two ligands used together. This is in accordance with research carried out by Jing et al.[36]

Cytotoxicity and Drug Combinations

Cytotoxicity of AP/Tf-Drn/Lut NPs was remarkably higher than single ligand–decorated AP-Drn/Lut NPs and Tf-Drn /Lut NPs ($P<0.05$, Figure 3). Both AP-Drn/Lut NPs and Tf-Drn/Lut NPs showed significantly **higher** cytotoxicity than

Table 2 Cellular uptake percentages (means ± SD, n=8)

Formulations	1 h	24 h
AP/Tf-Drn/Lut NPs	73.1±3.6	65.8±3.3
AP-Drn/Lut NPs	59.5±3.2	55.6±2.8
Tf-Drn/Lut NPs	57.1±2.9	54.2±3.1
AP-Drn NPs	60.2±3.3	53.1±2.6
Tf-Lut NPs	58.4±2.7	52.5±2.8
AP/Tf NPs	74.3±3.5	64.7±3.2

free Drn/Lut (P<0.05). Double drug–loaded AP/Tf-Drn/Lut NPs exhibited higher tumor cell–inhibition ability than single drug–loaded AP-Drn NPs and Tf-Lut NPs (P<0.05), which may be attributable to the synergic effect of the two drugs. To prove this, the CI_{50} values were calculated and are summarized in Table 3. Drn:Lut NPs at a ratio of 5:2 showed the lowest CI_{50} value (0.792) — the best synergic effect. Drn:Lut NPs at a ratio of 5:2 (w:w) were used for the preparation of the system.

In Vivo AML-Therapy Efficiency

Figure 4A shows that all drug-containing samples significantly suspended tumor growth compared with the saline control group (P<0.05). AP/Tf-Drn/Lut NPs exhibited the most remarkable AML-therapy efficiency compared with the single

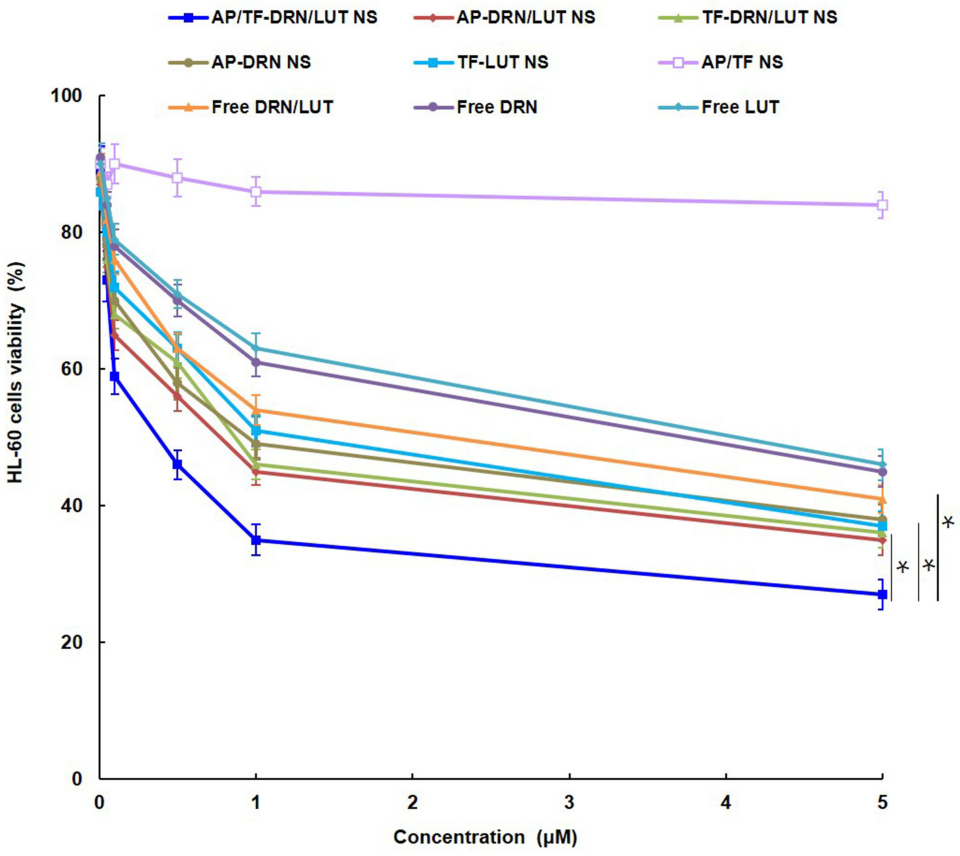

Figure 3 Cytotoxicity of AP/Tf-Drn/Lut NPs and other formulations evaluated with MTS assays.
Notes: Cytotoxicity of AP/Tf-Drn/Lut NPs was remarkably higher than single ligand–decorated NPs, single drug–loaded NPs, and free drugs. Data presented as means ± SD, n=6. *P<0.05.

Table 3 CI_{50} values of AP/Tf-Drn/Lut NPs when different Drn:Lut weight ratios were applied (means ± SD, n=8)

Formulations	Drn:Lut (w:w)	IC_{50} of Drn (μM)	IC_{50} of Lut (μM)	CI_{50}
AP-Drn NPs	/	0.93±0.09	/	/
Tf-Lut NPs	/	/	1.16±0.12	/
AP/Tf-Drn/Lut NPs	5:1	0.79±0.08	1.06±0.11	0.987
AP/Tf-Drn/Lut NPs	5:2	0.56±0.05	0.22±0.03	0.792
AP/Tf-Drn/Lut NPs	1:1	0.45±0.04	0.45±0.04	0.872
AP/Tf-Drn/Lut NPs	2:5	0.29±0.03	0.73±0.09	0.941
AP/Tf-Drn/Lut NPs	1:5	0.18±0.02	0.90±0.10	0.969

ligand–decorated, single drug–loaded, and free-drug groups (P<0.05). All the drug-loaded nanosystems illustrated greater AML-therapy efficiency than free-drug formulations (P<0.05). The body weight of mice did not significantly change when administered drug-containing formulations compared with reduction in body weight in the saline control and blank NP groups (P<0.05, Figure 4B). Mice treated with NPs showed negligible changes in ALT, Cre, and WBCs compared to the control group.

In Vivo Pharmacokinetics and Biodistribution

The pharmacokinetic parameters area under the plasma concentration–time curve (AUC), peak concentration (C_{max}), and terminal half-life ($t_{½}$) are summarized in Tables 4 and 5. Take the parameters for Lut as an example: the AUC of AP/Tf-Drn/Lut NPs (431.25±11.38 mg/L/h) was larger than that of AP-Drn/Lut NPs (311.26±8.34 mg/L/h), Tf-Drn/Lut NPs (289.86±7.65 mg/L/h), and free Drn/Lut (198.63±4.59 mg/L/h; P<0.05). As for Drn, C_{max} (55.36±3.21 L/kg/h) and $t_{½}$

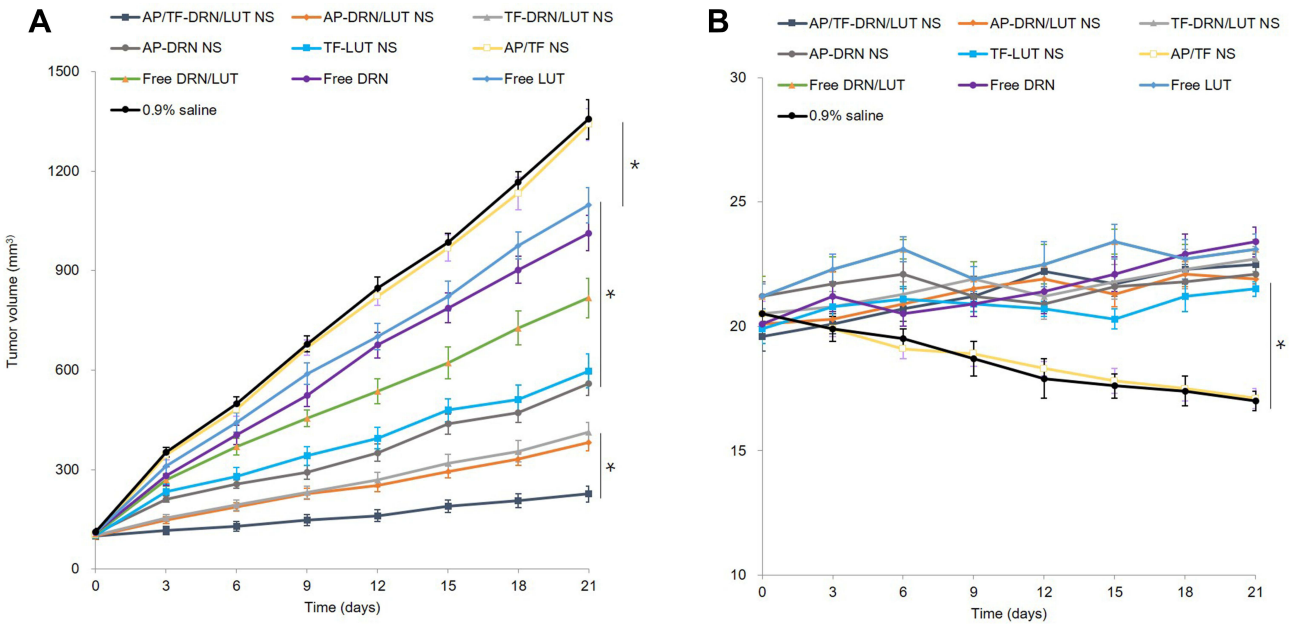

Figure 4 In vivo AML therapy efficiency: Tumor size (**A**) and body weight (**B**).
Notes: AP/Tf-Drn/Lut NPs exhibited the most remarkable AML therapy efficiency compared with single ligand–decorated, single drug–loaded and free-drug groups. Data presented as means ± SD, n=8. *P<0.05.

Table 4 Pharmacokinetic parameters for Drn (means ± SD, n=8)

Parameters	Unit	AP/Tf-Drn/Lut NPs	AP-Drn/Lut NPs	Tf-Drn/Lut NPs	Free Drn/Lut
C_{max}	L/kg/h	55.36±3.21*	42.31±2.98*	40.55±2.74*	29.83±2.88
$t_{1/2}$	h	12.37±0.78*	9.72±0.64*	8.84±0.53*	1.89±0.31
AUC_{0-t}	mg/L/h	659.72±19.56*	512.33±17.14*	488.75±21.16*	256.81±9.18
$AUC_{0-\infty}$	mg/L/h	662.31±20.05*	519.64±19.47*	493.23±22.44*	404.73±9.26

Note: *P<0.05 compared with free Drn/Lut.
Abbreviations: C_{max}, plasma drug peak concentration; $t_{1/2}$, half-life; AUC_{0-t}, area under curve of time 0 to last time point; $AUC_{0-\infty}$, area under curve of time 0 to maximum.

Table 5 Pharmacokinetic parameters for Lut (mean ± SD, n=8)

Parameters	Unit	AP/Tf-Drn/Lut NPs	AP-Drn/Lut NPs	Tf-Drn/Lut NPs	Free Drn/Lut
C_{max}	L/kg/h	35.47±3.18*	28.11±2.36*	26.59±2.95*	18.31±2.12
$t_{1/2}$	h	8.98±0.58*	5.46±0.41*	5.31±0.34*	1.51±0.29
AUC_{0-t}	mg/L/h	431.25±11.38*	311.26±8.34*	289.86±7.65*	198.63±4.59
$AUC_{0-\infty}$	mg/L/h	439.35±12.24*	317.64±11.35*	295.61±6.96*	202.34±5.13

Note: *P<0.05 compared with free Drn/Lut.
Abbreviations: C_{max}, peak plasma drug concentration; $t_{1/2}$, half-life; AUC_{0-t}, area under curve of time 0 to last time point; $AUC_{0-\infty}$, area under curve of time 0 to maximum.

(12.37±0.78 h) of AP/Tf-Drn/Lut NPs were significantly increased when compared with the other three samples. Drug distribution in tumor and other tissue samples are summarized in Figure 5. At both 1 and 48 h, AP/Tf-Drn/Lut NPs showed higher tumor-tissue distribution than single ligand–decorated AP-Drn/Lut NPs and Tf-Drn/Lut NPs (P<0.05),

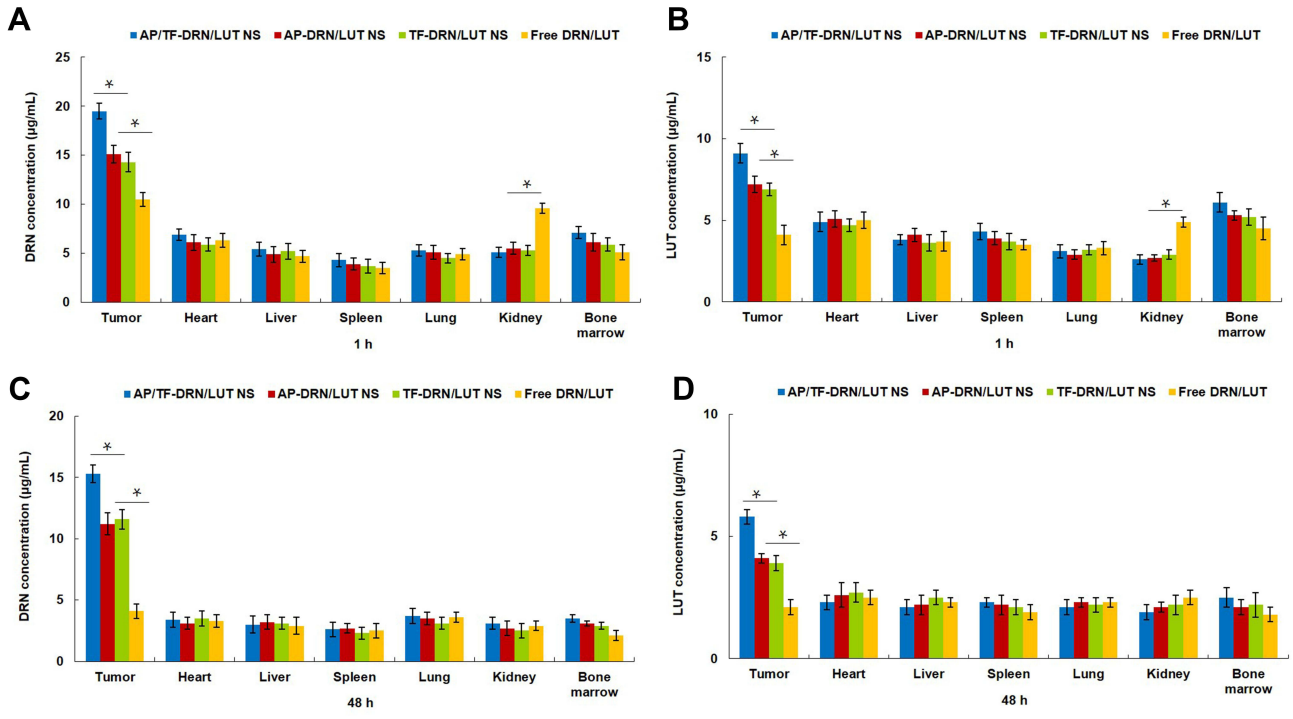

Figure 5 In vivo Drn (**A** and **C**) and Lut (**B** and **D**) distribution in tissue after 1 h (**A** and **B**) and 48 h (**C** and **D**) of drug administration. *P<0.05.
Notes: AP/Tf-Drn/Lut NPs showed higher tumor-tissue distribution than single ligand–decorated AP-Drn/Lut NPs, Tf-Drn/Lut NPs, and free Drn/Lut. Data presented as means ± SD, n=8. *P<0.05.

and the latter exhibited more tumor accumulation than free Drn/Lut ($P<0.05$). Meanwhile, free Drn/Lut had accumulated more in the kidney than drug-loaded nanosystems at 1 h ($P<0.05$).

Discussion

This study aimed to develop a AP- and Tf-codecorated Drn- and Lut-coloaded binary nanodrug-delivery system for AML therapy. Initially, AP- and Tf-containing ligands were designed and synthesized. Cationic AP-Drn NPs and anionic Tf-Lut NPs were prepared separately, then AP/Tf-Drn/Lut NPs were prepared by self-assembly through electronic interaction. Choueiri et al explained that changing the solvent composition or electrooxidation of ligands could control polymer–solvent interactions. These results expand the range of polymer ligands used for NP assembly and patterning, and can be used to explore new self-assembly modalities.[37] Yang et al developed pH/glutathione multiresponsive chitosan NPs, which were prepared by a self-assembly/self-cross-linking method. They concluded that this method could overcome the shortcomings of traditional methods, such as poor chemical stability, low loading efficiency, and single-responsive photosensitizer release.[38] Dong et al developed hyaluronic acid- and EGFR-targeted dual peptide ligand–modified docetaxel–formononetin NPs to facilitate prostate cancer therapy.[39] In the present research, we developed AP/Tf-Drn/Lut NPs for leukemia therapy.

AP/Tf-Drn/Lut NPs were 187 nm in size. Zhang et al said that particle sizes <200 nm could facilitate drug accumulation at tumor sites based on the enhanced permeability-and-retention effect, thereby reducing the drug dose and minimizing toxicity.[40] In vitro drug release is one of the significant properties of NPs and also of vital importance to drug ability. Pang et al developed hyaluronic acid–modified NPs for the delivery of erlotinib plus bevacizumab.[41] They found that the release behaviors of the two drugs loaded were similar, which was in line with the experiments in our research. In this study, we found that drug release from AP/Tf-Drn/Lut NPs was slower than single ligand (AP or Tf)–decorated systems, which could be construed as more ligands the surface of the NPs perhaps reducing the release rate. The decoration of ligands on the surface of NPs may affect drug-release behavior due to their hindering effect, as concluded by Dong et al.[39] The reason that drug release could not reach 100% may be due to the matrix of NPs hindering some drug release.

In vitro cytotoxicity of AP/Tf-Drn/Lut NPs was remarkably higher than single ligand–decorated AP-Drn/Lut NPs and Tf-Drn/Lut NPs. This phenomenon is due to the dual-ligand modification improving the targeting ability of the NPs, enhancing intracellular drug accumulation, and thus performing better in cancer therapy.[42] Double drug–loaded AP/Tf-Drn/Lut NPs exhibited higher tumor-cell inhibition than single drug–loaded AP-Drn NPs and Tf-Lut NPs, which may be attributable to the synergic effect of the two drugs. Li et al mentioned that when combination therapy is used in cancer chemotherapy, evaluation of the synergic effect is important and CI analyses are one of the most reliable methods.[43] The Chou–Talalay method was used to determine whether the drug-combination effect was synergic, additive, or antagonistic.[44] Drn:Lut at a ratio of 5:2 in the NPs had the lowest CI_{50} value (0.46), the best synergic effect, and was used for the preparation of the nanosystem.

In in vivo pharmacokinetic and biodistribution studies, AP/Tf-Drn/Lut NPs showed increased AUC, C_{max}, $t_{½}$, and tumor-tissue accumulation. Also, long circulating properties of nanosystems were observed, as discussed by Wang et al.[45] As reported by Jedrzejczyk et al, a Tf-containing conjugate can be used as a vehicle to increase drug concentration in leukemia cells overexpressing Tf receptors on their surface, which is also in accordance with the tumor accumulation observed in this study.[46] The dramatic increase accumulation in drug-loaded nanosystems in tumor tissue compared with free-drug solutions can be explained by the theory that solid tumors have leaky microvasculature and nanosized particles being able to passively target tumors owing to the enhanced permeability-and-retention effect.[47] Li et al also argued that less drug distribution in kidneys can decrease side effects and lead to better antitumor efficiency, which was achieved by the nanosystems in the present research.[48]

Nanosystems were reported by Zhu et al to overcome the side effects of conventional chemotherapeutic treatment and achieve high anticancer efficiency in vivo.[49] They used Tf-decorated NPs to strengthen the AML-inhibitory effects of drugs in a mouse model. He et al concluded that APs can bind to receptors on the cell membrane and mediate conjugated NPs to enter cells, which can served as ideal targeting ligands for AP-mediated drug-delivery systems for cancer therapy.[50] In this study, we found that AP/Tf-Drn/Lut NPs exhibited the best AML-therapy efficiency compared with

the single ligand–decorated, single drug–loaded, and free-drug groups. This was exactly the aim of this research, ie, dual ligands and drugs performing together. The body weight of mice was not significantly changed when administered drug-containing formulations, while the saline control group showed reduction in body weight. This was discussed by Wang et al: during treatment, mice may show a reduction in food intake, energy sag, and inactivity, leading to the reduction in body weight.[51] AP/Tf-Drn/Lut NPs in this study achieved both more efficient anticancer pharmacological activity with almost complete suppression of tumor growth and absence of toxicity related to weight loss, which was in line with the findings of Liu et al.[52]

Conclusion

In summary, AP/Tf-Drn/Lut NPs showed remarkably higher cytotoxicity than single ligand–decorated ones. Double drug–loaded AP/Tf-Drn/Lut NPs exhibited higher tumor-cell inhibition than single drug–loaded NPs, which showed the synergic effect of the two drugs. AP/Tf-Drn/Lut NPs achieved the most efficient antileukemic activity and absence of toxicity in vivo, and could be applied as a promising drug-delivery system for targeted treatment of leukemia, due to the synergic effect of the two drugs in this system. The limitations of this system include stability during large-scale production and application from bench to bedside.

Disclosure

The authors report no conflicts of interest.

References

1. Estey E, Döhner H. Acute myeloid leukaemia. *Lancet*. 2006;368(9550):1894–1907. doi:10.1016/S0140-6736(06)69780-8
2. Daver N, Schlenk RF, Russell NH, Levis MJ. Targeting FLT3 mutations in AML: review of current knowledge and evidence. *Leukemia*. 2019;33(2):299–312. doi:10.1038/s41375-018-0357-9
3. Huang X, Lin H, Huang F, et al. Targeting approaches of nanomedicines in acute myeloid leukemia. *Dose Response*. 2019;17(4):1559325819887048. doi:10.1177/1559325819887048
4. Ferrara F, Vitagliano O. Induction therapy in acute myeloid leukemia: is it time to put aside standard 3 + 7? *Hematol Oncol*. 2019;37(5):558–563. doi:10.1002/hon.2615
5. Lin M, Chen B. Advances in the drug therapies of acute myeloid leukemia (except acute wpromyelocytic leukemia). *Drug Des Devel Ther*. 2018;12:1009–1017. doi:10.2147/DDDT.S161199
6. Norsworthy KJ, Ko CW, Lee JE, et al. Mylotarg for treatment of patients with relapsed or refractory CD33-positive acute myeloid leukemia. *Oncologist*. 2018;23(9):1103–1108. doi:10.1634/theoncologist.2017-0604
7. Latagliata R, Breccia M, Fazi P, et al. Liposomal daunorubicin versus standard daunorubicin: long term follow-up of the GIMEMA GSI 103 AMLE randomized trial in patients older than 60 years with acute myelogenous leukaemia. *Br J Haematol*. 2008;143(5):681–689. doi:10.1111/j.1365-2141.2008.07400.x
8. Maakaron JE, Mims AS. Daunorubicin-cytarabine liposome (CPX-351) in the management of newly diagnosed secondary AML: a new twist on an old cocktail. *Best Pract Res Clin Haematol*. 2019;32(2):127–133. doi:10.1016/j.beha.2019.05.005
9. Lancet JE, Uy GL, Cortes JE, et al. CPX-351 (cytarabine and daunorubicin) liposome for injection versus conventional cytarabine plus daunorubicin in older patients with newly diagnosed secondary acute myeloid leukemia. *J Clin Oncol*. 2018;36(26):2684–2692. doi:10.1200/JCO.2017.77.6112
10. Kaspers GJ, Zimmermann M, Reinhardt D, et al. Improved outcome in pediatric relapsed acute myeloid leukemia: results of a randomized trial on liposomal daunorubicin by the international BFM study group. *J Clin Oncol*. 2013;31(5):599–607. doi:10.1200/JCO.2012.43.7384
11. Jin J, Wang FP, Wei H, Liu G. Reversal of multidrug resistance of cancer through inhibition of P-glycoprotein by 5-bromotetrandrine. *Cancer Chemother Pharmacol*. 2005;55(2):179–188. doi:10.1007/s00280-004-0868-0
12. Hu CM, Zhang L. Nanoparticle-based combination therapy toward overcoming drug resistance in cancer. *Biochem Pharmacol*. 2012;83(8):1104–1111. doi:10.1016/j.bcp.2012.01.008
13. Kim YS, Kim SH, Shin J, et al. Luteolin suppresses cancer cell proliferation by targeting vaccinia-related kinase 1. *PLoS One*. 2014;9(10):e109655. doi:10.1371/journal.pone.0109655
14. Chian S, Li YY, Wang XJ, Tang XW. Luteolin sensitizes two oxaliplatin-resistant colorectal cancer cell lines to chemotherapeutic drugs via inhibition of the Nrf2 pathway. *Asian Pac J Cancer Prev*. 2014;15(6):2911–2916. doi:10.7314/APJCP.2014.15.6.2911
15. Zheng CH, Zhang M, Chen H, et al. Luteolin from flos chrysanthemi and its derivatives: new small molecule Bcl-2 protein inhibitors. *Bioorg Med Chem Lett*. 2014;24(19):4672–4677. doi:10.1016/j.bmcl.2014.08.034
16. Danışman Kalındemirtaş F, Birman H, Candöken E, Bilgiş Gazioğlu S, Melikoğlu G, Kuruca S. Cytotoxic effects of some flavonoids and imatinib on the K562 chronic myeloid leukemia cell line: data analysis using the combination index method. *Balkan Med J*. 2019;36(2):96–105. doi:10.4274/balkanmedj.galenos.2018.2017.1244
17. Chen PY, Tien HJ, Chen SF, et al. Response of myeloid leukemia cells to luteolin is modulated by differentially expressed Pituitary Tumor-Transforming Gene 1 (PTTG1) oncoprotein. *Int J Mol Sci*. 2018;19(4):1173. doi:10.3390/ijms19041173
18. Polier G, Giaisi M, Köhler R, et al. Targeting CDK9 by wogonin and related natural flavones potentiates the anti-cancer efficacy of the Bcl-2 family inhibitor ABT-263. *Int J Cancer*. 2015;136(3):688–698. doi:10.1002/ijc.29009

19. Wang M, Wu H, Duan M, et al. SS30, a novel thioaptamer targeting CD123, inhibits the growth of acute myeloid leukemia cells. *Life Sci*. 2019;232:116663. doi:10.1016/j.lfs.2019.116663
20. Zhao N, Pei SN, Qi J, et al. Oligonucleotide aptamer-drug conjugates for targeted therapy of acute myeloid leukemia. *Biomaterials*. 2015;67:42–51. doi:10.1016/j.biomaterials.2015.07.025
21. Kim TH, Jo YG, Jiang HH, et al. PEG-transferrin conjugated TRAIL (TNF-related apoptosis-inducing ligand) for therapeutic tumor targeting. *J Control Release*. 2012;162(2):422–428. doi:10.1016/j.jconrel.2012.07.021
22. van Vlerken LE, Vyas TK, Amiji MM. Poly (ethylene glycol)-modified nanocarriers for tumor-targeted and intracellular delivery. *Pharm Res*. 2007;24(8):1405–1414. doi:10.1007/s11095-007-9284-6
23. Nguyen CT, Tran TH, Amiji M, Lu X, Kasi RM. Redox-sensitive nanoparticles from amphiphilic cholesterol-based block copolymers for enhanced tumor intracellular release of doxorubicin. *Nanomedicine*. 2015;11(8):2071–2082. doi:10.1016/j.nano.2015.06.011
24. Mao K, Zhang W, Yu L, Yu Y, Liu H, Zhang X. Transferrin-decorated protein-lipid hybrid nanoparticle efficiently delivers cisplatin and docetaxel for targeted lung cancer treatment. *Drug Des Devel Ther*. 2021;15:3475–3486. doi:10.2147/DDDT.S296253
25. El-Lakany SA, Elzoghby AO, Elgindy NA, Hamdy DA. HPLC methods for quantitation of exemestane–luteolin and exemestane–resveratrol mixtures in nanoformulations. *J Chromatogr Sci*. 2016;54(8):1282–1289. doi:10.1093/chromsci/bmw063
26. Yue Y, Eun JS, Lee MK, Seo SY. Synthesis and characterization of G5 PAMAM dendrimer containing daunorubicin for targeting cancer cells. *Arch Pharm Res*. 2012;35(2):343–349. doi:10.1007/s12272-012-0215-7
27. Wu R, Zhang Z, Wang B, et al. Combination chemotherapy of lung cancer - co-delivery of docetaxel prodrug and cisplatin using aptamer-decorated lipid-polymer hybrid nanoparticles. *Drug Des Devel Ther*. 2020;14:2249–2261. doi:10.2147/DDDT.S246574
28. Wu C, Xu Q, Chen X, Liu J. Delivery luteolin with folacin-modified nanoparticle for glioma therapy. *Int J Nanomedicine*. 2019;14:7515–7531. doi:10.2147/IJN.S214585
29. Fan X, Wang T, Ji Z, Li Q, Shen H, Wang J. Synergistic combination therapy of lung cancer using lipid-layered cisplatin and oridonin co-encapsulated nanoparticles. *Biomed Pharmacother*. 2021;141:111830. doi:10.1016/j.biopha.2021.111830
30. Haghighi FH, Binaymotlagh R, Mirahmadi-Zare SZ, Hadadzadeh H. Aptamer/magnetic nanoparticles decorated with fluorescent gold nanoclusters for selective detection and collection of human promyelocytic leukemia (HL-60) cells from a mixture. *Nanotechnology*. 2020;31(2):025605. doi:10.1088/1361-6528/ab484a
31. Chou TC. Drug combination studies and their synergy quantification using the Chou-Talalay method. *Cancer Res*. 2010;70(2):440–446. doi:10.1158/0008-5472.CAN-09-1947
32. Truebenbach I, Kern S, Loy DM, et al. Combination chemotherapy of L1210 tumors in mice with pretubulysin and methotrexate lipo-oligomer nanoparticles. *Mol Pharm*. 2019;16(6):2405–2417. doi:10.1021/acs.molpharmaceut.9b00038
33. Bao H, Zheng N, Li Z, Zhi Y. Synergistic effect of tangeretin and atorvastatin for colon cancer combination therapy: targeted delivery of these dual drugs using RGD peptide decorated nanocarriers. *Drug Des Devel Ther*. 2020;14:3057–3068. doi:10.2147/DDDT.S256636
34. Harris TJ, Green JJ, Fung PW, Langer R, Anderson DG, Bhatia SN. Tissue-specific gene delivery via nanoparticle coating. *Biomaterials*. 2010;31(5):998–1006. doi:10.1016/j.biomaterials.2009.10.012
35. Chen Y, Xu Z, Lu T, Luo J, Xue H. Prostate-specific membrane antigen targeted, glutathione-sensitive nanoparticles loaded with docetaxel and enzalutamide for the delivery to prostate cancer. *Drug Deliv*. 2022;29(1):2705–2712. doi:10.1080/10717544.2022.2110998
36. Jing F, Li J, Liu D, Wang C, Sui Z. Dual ligands modified double targeted nano-system for liver targeted gene delivery. *Pharm Biol*. 2013;51(5):643–649. doi:10.3109/13880209.2012.761245
37. Choueiri RM, Klinkova A, Pearce S, Manners I, Kumacheva E. Self-assembly and surface patterning of polyferrocenylsilane-functionalized gold nanoparticles. *Macromol Rapid Commun*. 2018;39(3). doi:10.1002/marc.201700554
38. Yang Z, Li P, Chen Y, et al. Construction of pH/glutathione responsive chitosan nanoparticles by a self-assembly/self-crosslinking method for photodynamic therapy. *Int J Biol Macromol*. 2021;167:46–58. doi:10.1016/j.ijbiomac.2020.11.141
39. Dong Z, Wang Y, Guo J, et al. Prostate cancer therapy using docetaxel and formononetin combination: hyaluronic acid and epidermal growth factor receptor targeted peptide dual ligands modified binary nanoparticles to facilitate the in vivo anti-tumor activity. *Drug Des Devel Ther*. 2022;16:2683–2693. doi:10.2147/DDDT.S366622
40. Zhang R, Ru Y, Gao Y, Li J, Mao S. Layer-by-layer nanoparticles co-loading gemcitabine and platinum (IV) prodrugs for synergistic combination therapy of lung cancer. *Drug Des Devel Ther*. 2017;11:2631–2642. doi:10.2147/DDDT.S143047
41. Pang J, Xing H, Sun Y, Feng S, Wang S. Non-small cell lung cancer combination therapy: hyaluronic acid modified, epidermal growth factor receptor targeted, pH sensitive lipid-polymer hybrid nanoparticles for the delivery of erlotinib plus bevacizumab. *Biomed Pharmacother*. 2020;125:109861. doi:10.1016/j.biopha.2020.109861
42. Wang H, Sun G, Zhang Z, Ou Y. Transcription activator, hyaluronic acid and tocopheryl succinate multi-functionalized novel lipid carriers encapsulating etoposide for lymphoma therapy. *Biomed Pharmacother*. 2017;91:241–250. doi:10.1016/j.biopha.2017.04.104
43. Li S, Wang L, Li N, Liu Y, Su H. Combination lung cancer chemotherapy: design of a pH-sensitive transferrin-PEG-Hz-lipid conjugate for the co-delivery of docetaxel and baicalin. *Biomed Pharmacother*. 2017;95:548–555. doi:10.1016/j.biopha.2017.08.090
44. Chou TC. Theoretical basis, experimental design, and computerized simulation of synergism and antagonism in drug combination studies. *Pharmacol Rev*. 2006;58(3):621–681. doi:10.1124/pr.58.3.10
45. Wang B, Hu W, Yan H, et al. Lung cancer chemotherapy using nanoparticles: enhanced target ability of redox-responsive and pH-sensitive cisplatin prodrug and paclitaxel. *Biomed Pharmacother*. 2021;136:111249. doi:10.1016/j.biopha.2021.111249
46. Jedrzejczyk M, Wisniewska K, Kania KD, Marczak A, Szwed M. Transferrin-bound doxorubicin enhances apoptosis and DNA damage through the generation of pro-inflammatory responses in human leukemia cells. *Int J Mol Sci*. 2020;21(24):9390. doi:10.3390/ijms21249390
47. Choi J, Ko E, Chung HK, et al. Nanoparticulated docetaxel exerts enhanced anticancer efficacy and overcomes existing limitations of traditional drugs. *Int J Nanomedicine*. 2015;10:6121–6132. doi:10.2147/IJN.S88375
48. Li C, Ge X, Wang L. Construction and comparison of different nanocarriers for co-delivery of cisplatin and curcumin: a synergistic combination nanotherapy for cervical cancer. *Biomed Pharmacother*. 2017;86:628–636. doi:10.1016/j.biopha.2016.12.042
49. Zhu B, Zhang H, Yu L. Novel transferrin modified and doxorubicin loaded pluronic 85/lipid-polymeric nanoparticles for the treatment of leukemia: in vitro and in vivo therapeutic effect evaluation. *Biomed Pharmacother*. 2017;86:547–554. doi:10.1016/j.biopha.2016.11.121

50. He F, Wen N, Xiao D, et al. Aptamer-based targeted drug delivery systems: current potential and challenges. *Curr Med Chem*. 2020;27 (13):2189–2219. doi:10.2174/0929867325666181008142831
51. Wang L, Wang W, Rui Z, Zhou D. The effective combination therapy against human osteosarcoma: doxorubicin plus curcumin co-encapsulated lipid-coated polymeric nanoparticulate drug delivery system. *Drug Deliv*. 2016;23(9):3200–3208. doi:10.3109/10717544.2016.1162875
52. Liu B, Han L, Liu J, Han S, Chen Z, Jiang L. Co-delivery of paclitaxel and TOS-cisplatin via TAT-targeted solid lipid nanoparticles with synergistic antitumor activity against cervical cancer. *Int J Nanomedicine*. 2017;12:955–968. doi:10.2147/IJN.S115136